METHOD FOR FORECASTING THE OPTICAL CHARACTERISTICS OF THE PERTURBED AEROSOL–CLOUDY ATMOSPHERE

V.S. Komarov, S.A. Soldatenko, and A.N. Borisov

Institute of Atmospheric Optics,
Siberian Branch of the Russian Academy of Sciences, Tomsk
Received December 28, 1994

Simulation system is considered in the paper, which includes models of the atmosphere and impurity transport. The system is intended for simulation of the dynamics of cloudy fields and anthropogenic aerosol in order to provide the opto–electronic systems for Earth observation from space with meteorological data. The system under consideration has been used for forecasting the optical thickness and horizontal size of smoke aerosol clouds. Some results obtained using this system are presented.

1. INTRODUCTION

Effective operation of the atmospheric adaptive opto–electronic systems of different end use installed onboard air and space platforms, strongly depends on sufficiently complete and prompt information about the physical state of the atmospheric optical channel (AOC). The optical signal transfer through the atmosphere is known[1–3] to be accompanied by internal and external noise reducing the AOC information–transfer characteristics. Omitting the analysis of sources of internal noise connected with the operation of transceiving equipment, let us note that external noise is mainly due to the atmospheric conditions, such as cloudiness, fog, haze, dense aerosol clouds of natural and anthropogenic origin,[1] which may change qualitatively the character of optical signal propagation in the atmosphere.

The model imitating the processes of global Earth–observational system operation (see, e.g., Refs. 4–6) allowed one, on the one hand, to evaluate the efficiency of operation of these systems under various atmospheric conditions and, on the other hand, to compile the list of atmospheric parameters and conditions to be taken into account both at the design and at the stage of planning the use of airborne and spaceborne opto–electronic systems. As the analysis shows, natural cloudiness and dense aerosol clouds (AC), including smoke and dust, which screen the Earth's surface and limit the potentials of opto–electronic observational systems, most strongly affect the Earth observations. This means that to supply meteorological information at the stage of current planning of the operation of the global Earth–observational systems, the actual and predicted data are needed, especially, about natural cloudiness and dense aerosol clouds (their thickness, horizontal size, altitudes of their top and base, optical thickness, microphysical characteristics, type of natural cloudiness).

Note that dense aerosol clouds (smoke, dust, soot) may occur not only due to natural events (large forest fires, dust and sand storms) but also as a result of local and regional wars[7,8] (for example, the armed conflict between Iraq and Kuwait).

The present paper is aimed at consideration of the main characteristics of the system for simulating and predicting the dynamic of cloud fields and aerosol formations of anthropogenic origin in order to solve the problems on provision of opto–electronic systems for global Earth observation with meteorological data.

The imitation system proposed here includes two interrelated large–scale models. The first one is based on complete (primitive) equations of the hydrothermodynamics of the atmosphere. The second one is based on the equation of passive impurity transport in the atmosphere. The first model is used for prediction of the main thermodynamic characteristics of the atmosphere (velocity components u and v of motion along x and y axes, vertical velocity, temperature T, mass fraction of water vapor q, characteristics of cloudiness), which are the input parameters for the second model, at the regular grid nodes. The second model is intended to describe the dynamics of AC in the atmosphere and thus to find the spatiotemporal distribution of the atmospheric optical thickness τ in the visible and near–IR spectral ranges.

2. HYDRODYNAMIC MODEL OF THE ATMOSPHERE

Using designations, common in meteorology, equations of the model in the modified σ coordinate system allowing for the scale factor of a map in stereographic projection are as follows:

$$\frac{\mathrm{d}\pi u}{\mathrm{d}t} = \pi f^* v - m\pi\left(\frac{\partial\Phi}{\partial x} + c_p\,\theta\,\frac{\partial P^{R/c_p}}{\partial x}\right) + \pi F_u - g\frac{\partial \mathrm{t}_x}{\partial \mathrm{s}}; \quad (1)$$

$$\frac{\mathrm{d}\pi v}{\mathrm{d}t} = -\pi f^* u - m\pi\left(\frac{\partial\Phi}{\partial y} + c_p\,\theta\,\frac{\partial P^{R/c_p}}{\partial y}\right) + \pi F_v - g\frac{\partial \mathrm{t}_y}{\partial \mathrm{s}}; \quad (2)$$

$$\frac{\partial\pi}{\partial t} = -m^2\left(\frac{\partial\pi u}{\partial x} + \frac{\partial\pi v}{\partial y}\right) - \frac{\partial\pi\dot{\sigma}}{\partial\sigma}; \quad (3)$$

$$\frac{\mathrm{d}\pi\theta}{\mathrm{d}t} = \pi F_\theta + \frac{g}{c_p}\frac{\partial H}{\partial\sigma} + \pi(\varepsilon_r + \varepsilon_\Phi); \quad (4)$$

$$\frac{\partial\Phi}{\partial\sigma} = -c_p\,\theta\,\frac{\partial P^{R/c_p}}{\partial\sigma}; \quad (5)$$

$$\frac{\mathrm{d}\pi q}{\mathrm{d}t} = \pi F_q + g\frac{\partial E}{\partial\sigma} + \pi M, \quad (6)$$

where

$$\frac{\mathrm{d}\pi a}{\mathrm{d}t} = \frac{\partial\pi a}{\partial t} + m^2\left[\frac{\partial\pi u^* a}{\partial x} + \frac{\partial\pi v^* a}{\partial y}\right] + \frac{\partial\pi\dot{\sigma} a}{\partial\sigma}. \quad (7)$$

In Eqs. (1)–(7) the following designations are used: $\sigma = (p - p_\mathrm{t})/\pi$, $\pi = p_\mathrm{s} - p_\mathrm{t}$ (p_s is the pressure near the

0235-6880/95/07 534-04 $02.00

Earth's surface and p_t = 100 hPa is the pressure at the top of the model atmosphere), $\dot{\sigma}$ is an analog of vertical velocity, Φ is the geopotential, θ is the potential temperature, F_u and F_v are the rates of momentum variation due to Reynolds stress, τ_x and τ_y are the components of the vector of vertical turbulent flux of momentum, $f^* = f + u(\partial m/\partial y) - v(\partial m/\partial x)$ (f is the Coriolis parameter), $P = p/P_0$ (P_0 = 1000 hPa), F_θ and F_q are the rates of change of potential temperature and mass fraction of water vapor due to horizontal turbulent diffusion, H and F are the vertical turbulent fluxes of heat and water vapor, ε_r and ε_Φ are the radiant and phase inflows of heat, and M is the inflow (outflow) of water vapor.

The set of equations (1)–(6) is solved in the region being a square inscribed in the equatorial latitudinal circle in the map of stereografic projection (grid step is 300 km at latitude of 60°). To describe the dynamics of ACs at the initial stage of their evolution, the model may be telescoped[9]: one or several grids are placed within the square, each being rectangular in shape and spanning the territory of $(6.5\times7.5)\cdot10^3$ km with 150 km step at the latitude of 60°.

Boundary conditions along the vertical coordinate are imposed as usual and provide a conservation of total mass of the atmosphere: $\dot{\sigma}$ =0 at σ = 1 and σ = 0 (see Ref. 10). At the lateral boundaries of the external region the boundary conditions are imposed so that the set has a unique solution and is physically closed:

$$V^{(n)} = \partial V^{(\tau)} / \partial n = \partial T / \partial t = \partial q / \partial t = 0 , \qquad (8)$$

where $V^{(n)}$ and $V^{(\tau)}$ are velocity components, normal and tangential to lateral boundaries, and n is the normal to the lateral boundary.

The lateral boundary conditions for inscribed grids are specified with regard to results obtained in Ref. 11: in the near–boundary zone of width 500 km the approximation of viscous absorption (the artifical viscosity with large viscosity coefficient of 10^6 m^2/s is introduced) and weighted tendentions (time derivatives) are used.

The main physical processes, which engender energy sinks and sources in the atmosphere, are parametrized in the model, namely, the processes of radiant energy transfer, phase transformations of atmospheric moisture, cloudiness, convection and convective precipitations, atmospheric interaction with the underlying surface, vertical and horizontal turbulent exchange.[12] The algorithm is refined in order to take into account the processes of radiation absorption and scattering by anthropogenic aerosol.[13] According to Ref. 13, the total (direct and scattered) downwelling radiation flux at the lower boundary of a layer of strongly absorbing aerosol is given by the equation

$$F_\Sigma(\tau_a) = I'_0 \mu_0 R(\tau_a, \omega_a, g_a, \mu_0) , \qquad (9)$$

where $R(\tau_a, \omega_a, g_a, \mu_0) = \exp[-k(\omega_a, g_a)\tau_a / \mu_0]$, I'_0 is the flux of downwelling solar radiation at the upper boundary of a layer, μ_0 is the cosine of solar zenith angle, ω_a is the single scattering albedo, g_a is the mean cosine of scattering phase function, and τ_a is the optical thickness of an AC. The coefficient $k(\omega_a, g_a)$ is approximately equal to

$$k(\omega_a, g_a) = 1 - c\, g_a^n\, \omega_a . \qquad (10)$$

Here c and n are the parameters found by the least–square fitting over a wide range of ω_a and g_a values. In Ref. 13 this parameters were found to be c = 0.97 and n = 0.26.

Quite simple analytical dependence

$$A(\tau_a) = A_\infty \{1 - \exp[-a\, k(\omega_a, g_a)\, \tau_a / \mu_0]\} \qquad (11)$$

is used to calculate the albedo of aerosol layer, where A_∞ is the albedo of semi–infinite layer, calculated by the equation

$$A_\infty = 1 - \varphi(\omega_a, \mu_0) \sqrt{1 - \omega_a} . \qquad (12)$$

In Eqs. (11) and (12) the following designations are used: a for experimentally fitted parameter and $\varphi(\omega_a, \mu_0)$ for the Ambartsumyan function approximately equal to

$$\varphi(\omega_a, \mu_0) = \exp[0.022 - 0.29\, \mu_0^{0.52} \ln(1 - \omega_a)] . \qquad (13)$$

In Eqs. (12) and (13) it is appropriate to use the "transport" value of the photon survival probability[13]:

$$\omega_t = \omega_a (1 - g_a) / (1 - g_a \omega_a) . \qquad (14)$$

The approach considered based on simple exponential approximation for solar radiation transmission and scattering by the layer of strongly absorbing aerosol yields the results close to those obtained by delta–Eddington method for practically any aerosol of noncondensation origin (for example, dust or smoke) and for strongly polluted haze (such as arctic one) at solar zenith angles close to the average climatic values.

The set of equations (1)–(6) with the initial and boundary conditions prescribed is integrated numerically using the splitting method,[14] according to which the problem is splitted into two stages, i.e., the advection and adaptation stages. At the first stage (advection) the equations are integrated with the use of two–step Laks–Vendroff scheme, whereas at the second stage – with the "back–and–forth" scheme with implicit representation of Coriolis terms.[15]

3. MODEL OF POLUTION TRANSPORT

The model describing the aerosol dynamic in the atmosphere is based on the known transport equation[16]

$$\frac{\partial \pi c}{\partial t} = -m^2\left[\frac{\partial}{\partial x}\left(\frac{\pi u c}{m}\right) + \frac{\partial}{\partial y}\left(\frac{\pi v c}{m}\right)\right] - \frac{\partial \pi \dot{\sigma} c}{\partial \sigma} +$$

$$+ \pi F_c + g \frac{\partial Q_c}{\partial \sigma} + \pi (I_c + f_c) , \qquad (15)$$

where c is the number density of a contaminant under consideration, Q_c is the vertical turbulent flux of the contaminant, F_c is the rate of the contaminant transformation due to horizontal turbulent mixing, I_c is the term accounting for sedimentation, wash out, and self–induced vertical rise due to absorption of solar radiation by aerosol,[17] and f_c is the source function.

Since equation (15) describes the functions with large spatial gradients and discontinuities of the first order, the total variation diminishing (TVD) scheme[18] is used for its numerical solution.

Up to date a lot of numerical schemes belonging to the TVD class were elaborated. We use in our model a

relatively simple numerical scheme. For the single–dimension transport equation it has the form

$$c_i^{n+1} = c_i^n - u\frac{\Delta t}{\Delta x}(c_i^n - c_{i-1}^n) - (f_{i+1/2}^n - f_{i-1/2}^n). \quad (16)$$

Here i is the number of a step in space, n is the number of a step in time, Δt and Δx are steps in time and space, and $f_{i+1/2}^n = \varphi(r_i)\, u\frac{\Delta t}{\Delta x}\left(1 - u\frac{\Delta t}{\Delta x}\right)(c_{i+1}^n - c_i^n)$. The computational flux $f_{i-1/2}^n$ is defined similarly. The function $\varphi(r_i)$ is referred to as a bounding function, and its argument is defined as the ratio of gradients

$$r_i = \frac{(c_i - c_{i-1})}{(c_{i+1} - c_i)}.$$

So the bounding function is set as follows:

$$\varphi(r) = \begin{cases} \min(2,\ r) & \text{at } r > 1, \\ \min(2r,\ 1) & \text{at } 0 < r \le 1, \\ 0 & \text{at } r \le 0, \end{cases} \quad (17)$$

thus providing the conditions of total variation diminishing.[18]

The processes of sedimentation, wash out, and self–induced vertical rise are parametrized in the model following the schemes considered in Ref. 19.

Since atmospheric aerosols of anthropogenic origin are polydisperse, the equation of the type (15) is used to describe the contaminant evolution separately for each fraction. Within a fraction the particle radius is considered to be constant. To this end the particle size spectrum is first divided into fractions. The number of fractions is limited mainly by the computational capacities.

4. RESULTS OF NUMERICAL EXPERIMENTS

The model of the atmosphere and the model of contaminant transport comprise a unitary simulation system, operating in an interactive mode. When the results of objective analysis and preliminary initialization of meteorological fields as well as the initial values of characteristics of aerosol formations and aerosol sources are fed to the system input, the set of equations (1)–(6) and (15) with the preset boundary conditions can be solved numerically, and thus the main regularities of evolution of natural and anthropogenic aerosol formations in the atmosphere can be revealed and the basic optical characteristics, required for solving the problems of supplying the system of global Earth observation with meteorological data, can be forecasted.

The evaluation of the model quality obtained and preliminary results of numerical experiments show[11] that the simulation system proposed allows forecasting of the AC dynamics for sufficiently long period (up to one month and even longer), however, this forecast is informative only during 5–6 days for certain objective reasons.

From the point of view of solving the problems of the meteorological data provision to the systems of global Earth observation equipped with opto–electronic devices, the study of dynamics of the main AC characteristics, having an effect on the radiation transfer in the visible and near–IR, is of great interest. Among such characteristics are, first of all, the optical thickness τ and horizontal size of an AC. In order to reveal the main regularities in AC optical thickness and horizontal size changes in time, the test numerical experiments with an isolated smoke clouds were performed.

The initial characteristics of aerosol formations are specified based on the type of a fire and taking into account the stores of combustible materials and available evaluation of smoke output.

If the one half of stores of potential combustibles in a city with population of one million is burnt, the mass of smoke evolved is about 0.2 Mt (Ref. 8). Since the rate of energy emission at city fires is rather high, the smoke from it rises up to the tropopause level. The total mass of the smoke arising by combustion of city buildings is calculated based on a known number of city fires.

Let us consider the situation when the smoke originating from forest fires enters the atmosphere. The stores of dry wood in a forest are estimated[8] to be 15 kg/m^2. In forest fires about 30% of dry biomass are burnt out, i.e., about 5 kg of material per 1 m^2 of a forest. With the smoke output of 2% (Ref. 7), its mass, evolved as a result of combustion of biomass from 1 m^2, equals to 0.1 kg. So the smoke mass from an isolated forest fire over the area of $2.5 \cdot 10^4$ km^2 comprises 0.25 Mt. Usually the smoke from forest fires rises up to the altitude of 2–3 km, and forest fires are significantly more prolonged than the city ones. These pecularities should be taken into account in formulating the initial characteristics of ACs.

Let us now turn our attention to the consideration of the results of numerical experiments. Initial meteorological fields corresponded to the real situation taking place at 00 (03) hr July 19, 1979.

Figure 1 shows the evolution of horizontal size of a typical AC originating from the city fire for two different values of boundary optical thickness, τ_b. As follows from the figure, the area of AC grows up for about five days (for $\tau_b = 1$) due to advective transport and turbulence and then rapidly vanishes. The sharp decrease in τ (see Fig. 2) in this case is caused by the action of different physical mechanisms, engendering the AC dynamics.

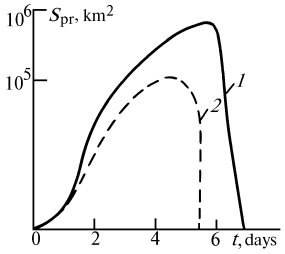

FIG. 1. The area of projection S_{pr} of a separate smoke cloud from a city fire vs. time for $\tau_b = 1$ (1) and 3 (2), $\lambda = 0.55$ μm.

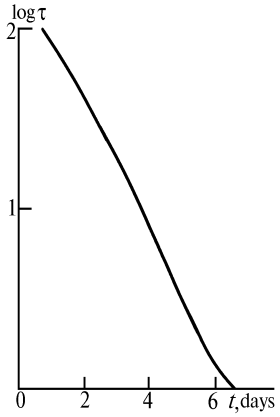

FIG. 2. The optical thickness of a separate smoke cloud from a city fire vs. time for $\lambda = 0.55$ μm.

To illustrate the possibility of forecasting the conditions of Earth observations, we consider the following hypothetical scenario of a smoke emission into the atmosphere. Regions with the size 10°×10° are enumerated in Fig. 3. Table I presents the number and types of fires in each region. The total number of city fires is 103, and the number of forest fires is 23. The mass of smoke entering the atmosphere from city fires is, according to conclusions presented above, 20.6 Mt, and that from the forest fires is 5.6 Mt. Thus, the total mass of smoke emitted into the atmosphere is 26.2 Mt.

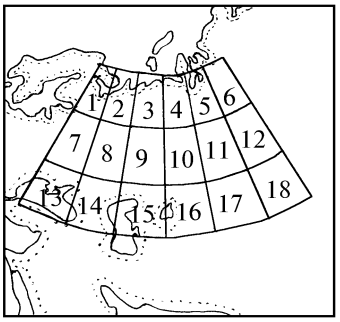

FIG. 3. The regions under study.

Being formed, the smoke clouds have the optical thickness of tens or even hundreds of units, and, therefore, they present an impenetrable barrier to optical radiation over the entire optical range. At the same time, the coefficient of covering individual regions is relatively small (about 1%).

Futher in time separate ACs spread and merge thus widening the area of a smoke AC projection S_{pr} onto the Earth's surface. At the same time the optical thickness of ACs significantly decreases. As an example, Fig. 4 presents the evolution of the coefficient of covering of some regions by ACs. The coefficients obtained may be used to evaluate the efficiency of an optical observational system installed onboard air or space platforms.

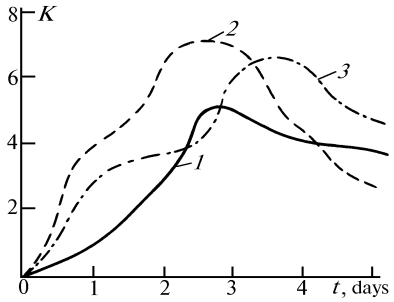

FIG. 4. The coefficient of covering by smoke clouds, K: regions No. 8 *(1),* No. 9 *(2), and* No. 12 *(3).*

TABLE I. The number and type of fires in regions.

Region current number	1	2	3	4	5	6	7	8	9	10	11	12	13	14	15	16	17
Number of city fires	0	0	2	1	3	0	10	10	10	15	10	10	5	10	5	5	2
Number of forest fires	0	0	1	1	1	0	2	2	3	4	2	2	1	2	1	1	0

REFERENCES

1. V.E. Zuev and M.V. Kabanov, *Transfer of Optical Signals in the Earth's Atmosphere (under Conditions of Noise)* (Sov. Radio, Moscow, 1977), 368 pp.
2. V.E. Zuev, B.D. Belan, and G.O. Zadde, *Optical Weather* (Nauka, Novosibirsk, 1990), 191 pp.
3. Yu. G. Yakushenkov, *Theory and Calculation of Opto–Electronic Devices* (Mashinostroenie, Moscow, 1989), 359 pp.
4. V.T. Bobrovnikov, Issled. Zemli iz Kosmosa, No. 1, 83–89 (1981).
5. E.A. Gorbushina and V.A. Kottsov, Issled. Zemli iz Kosmosa, No. 1, 78–82 (1981).
6. J.R. Greeves, J. Appl. Meteorol. **12**, No. 1, 12–22 (1973).
7. K.Ya. Kondrat'ev, *Natural and Anthropogenic Climate Changes* (VINITI, Moscow, 1986), 349 pp.
8. M.I. Budyko, G.S. Golitsyn, and Yu.A. Israel', *Global Climate Catastrophes* (Gidrometeoizdat, Moscow, 1986), 158 pp.
9. A. Sandrem and T. Elvius, in: *Numerical Methods Used in Atmospheric Models* (Gidrometeoizdat, Leningrad, 1982), pp. 274–302.
10. P.N. Belov, E.P. Borisenkov, and B.D. Panin, *Numerical Methods of Weather Forecasting* (Gidrometeoizdat, Leningrad, 1989), 376 pp.
11. S.A. Soldatenko, Izv. RAN, Fiz. Atmos. Okeana **28**, No. 2, 115–127 (1992).
12. Yu.G. Lushev and S.A. Soldatenko, Tr. LGMI, No. 85, 25–36 (1985).
13. A.S. Ginzburg and I.N. Sokolin, Izv. Akad. Nauk SSSR, Fiz. Atmos. Okeana **25**, No. 9, 954–959 (1989).
14. V.V. Penenko, *Methods for Numerical Simulation of Atmospheric Processes* (Gidrometeoizdat, Leningrad, 1981), 351 pp.
15. S.A. Soldatenko, Meteorol. Gidrol., No. 5, 90–100 (1985).
16. L.T. Matveev, *Principles of General Meteorology. Atmospheric Physics* (Gidrometeoizdat, Leningrad, 1965), 869 pp.
17. P.F. Demchenko and A.S. Ginsburg, Meteorol. Gidrol., No. 8, 51–57 (1986).
18. A. Harten, J. Comp. Phys. **49**, No. 3, 304–357 (1983).
19. S.A. Soldatenko and O.M. Sobolevskii, Atmos. Oceanic Opt. **7**, No. 2, 112–116 (1994).